JOURNAL OF GEOPHYSICAL RESEARCH, VOL. 108, NO. B9, 2434, doi:10.1029/2001JB000703, 2003

# Estimate of heat flux and its temporal variation at the TAG hydrothermal mound, Mid-Atlantic Ridge 26°N

Shusaku Goto[1] and Masataka Kinoshita[2]
School of Marine Science and Technology, Tokai University, Shimizu, Shizuoka, Japan

Adam Schultz
School of Earth Sciences, Cardiff University, Cardiff, UK

Richard P. Von Herzen
Woods Hole Oceanographic Institution, Woods Hole, Massachusetts, USA

Received 22 June 2001; revised 11 April 2003; accepted 10 June 2003; published 17 September 2003.

[1] From August 1994 to March 1995, three 50-m-high vertical thermistor arrays designated "Giant Kelps" (GKs) were deployed around the central black smoker complex (CBC) at the TAG hydrothermal mound, Mid-Atlantic Ridge (26°08′N, 44°49′W). These were designed to monitor the temporal variability of the vertical temperature distribution in the hydrothermal plume. One small high-temperature probe "Hobo" was also deployed in one of the black smoker vents of CBC. Over the observation period, two typical characteristics are recognized in plume temperatures measured with GKs: (1) the amplitudes of temperature anomalies decrease with increasing height above the top of CBC; (2) maximum temperature anomalies on the upper thermistors occurred periodically and nearly simultaneously across the array about every 6 hours. Conversely, maximum temperature anomalies on the lower thermistors occurred periodically every 12 hours, indicating that the location of the plume discharged from CBC was forcibly moved by the change in direction of tidally modulated current flow. The heat flux from CBC was estimated from temperatures measured by GKs based on a model of buoyant hydrothermal fluid rising in a stable, stratified density environment. The estimated heat flux from CBC gradually decreases from about 86 to 55 MW over the ~7 months of measurement, with a mean rate of decrease of 0.17 MW $d^{-1}$. Since the black smoker effluent temperature measured with Hobo was almost stable over the measurement period, a plausible cause of the decrease is a reduction in the volume of hydrothermal fluid provided to the CBC (in which case the estimated mean rate of decrease in volume flux of CBC is 8.9 $m^3$ $d^{-1}$). Estimated heat flux, temperature anomalies observed by Hobo, and diffuse flow and subbottom temperature anomalies recorded by other long-term monitoring instruments before, during, and after ODP Leg 158 indicate that the drilling probably affected the fluid flow pattern within the mound but had little effect on the total heat flux from CBC. *INDEX TERMS:* 3015 Marine Geology and Geophysics: Heat flow (benthic) and hydrothermal processes; 3094 Marine Geology and Geophysics: Instruments and techniques; 4832 Oceanography: Biological and Chemical: Hydrothermal systems; 8135 Tectonophysics: Hydrothermal systems (8424); 8424 Volcanology: Hydrothermal systems (8135); *KEYWORDS:* heat flux, hydrothermal plume, TAG hydrothermal mound

**Citation:** Goto, S., M. Kinoshita, A. Schultz, and R. P. Von Herzen, Estimate of heat flux and its temporal variation at the TAG hydrothermal mound, Mid-Atlantic Ridge 26°N, *J. Geophys. Res.*, *108*(B9), 2434, doi:10.1029/2001JB000703, 2003.

## 1. Introduction

[2] Manned submersible and remotely operated vehicle observations over the past two decades have revealed submarine hydrothermal activity at many mid-ocean ridge sites and have provided constraints on the evolution of magmatic, tectonic, and chemical processes underlying surface expressions of venting [e.g., *Fornari and Embley*, 1995]. The magnitude of the heat source and the local crustal permeability distribution are probably the most important parameters

[1]Earthquake Research Institute, University of Tokyo, Bunkyo-ku, Tokyo, Japan.
[2]Japan Marine Science and Technology Center, Yokosuka, Kanagawa, Japan.


0148-0227/03/2001JB000703$09.00

controlling the spatial extent, magnitude, and characteristics of seafloor hydrothermal activity. Estimates of advective heat flux carried by hydrothermal effluent provide quantitative information on these parameters.

[3] *Macdonald* [1980] first estimated the heat flux from a black smoker vent on the East Pacific Rise (EPR) at 21°N as 250 ± 80 MW by direct measurements of effluent flow rate, temperature, and the vent orifice dimension. *Converse et al.* [1984] measured vent orifice dimensions, flow rates, and fluid temperatures 3–5 cm above the vent orifices at hydrothermal sites at EPR 21°N. Applying a model of plume development, they estimated heat flux for individual vents as 0.5–10 MW. *Little et al.* [1987] used a vertical array of thermistors and a current meter to measure temperatures and velocities within plumes and estimated the heat flux of a single vent as 3.7 ± 0.8 MW at a hydrothermal site on the EPR 11°N, using a simple plume model based on the work of *Fischer et al.* [1979]. *Bemis et al.* [1993] measured temperatures and velocities within rising plumes with a thermistor array system similar to that of *Little et al.* [1987] and estimated heat flux of 0.1–75 MW for vents at the Endeavour and Cleft segments of the Juan de Fuca Ridge. At the same hydrothermal sites, *Ginster et al.* [1994] directly measured exit temperature, flow rate, and vent orifice dimension, and estimated heat flux for individual vents as 0.1–94 MW.

[4] Long-term monitoring has provided direct evidence for temporal variability of hydrothermal activity. *Fornari et al.* [1998] monitored vent fluid temperature at the Bio9 vent at EPR 9°51′N for 3 years and measured an abrupt increase in temperature from 365° to 373°C. Since a seismic swarm commenced beneath the vent 4 days before the temperature anomaly, they concluded that the temperature anomaly was caused by cracking of hot crustal rock associated with the evolution of the hydrothermal system following the 1991–1992 eruptions. *Schultz et al.* [1992] monitored temperature and velocity of diffuse fluid for 46 days at the Endeavour segment of the Juan de Fuca Ridge and indicated that the fluid temperature modulated at semidiurnal tidal period.

[5] In order to estimate heat flux and its temporal variation at the central black smoker complex (CBC) at TAG hydrothermal mound, three vertical thermistor arrays and one long-term high-temperature monitoring probe were deployed to monitor plume temperatures from August 1994 to March 1995 [*Kinoshita et al.*, 1996, 1998]. During these observations, Ocean Drilling Program Leg 158 drilled 17 holes at the TAG hydrothermal mound [*Humphris et al.*, 1995]. Therefore the flux measurements occurred before, during, and after drilling. The observations reported here were part of a large-scale instrumentation campaign by Japanese, American, British, and Russian scientists to obtain baseline observations of TAG hydrology, geology, and biology prior to drilling, to study natural time variations of these processes, and to gauge the impact of drilling on the TAG system. Many of these results have been reported elsewhere. In this paper, we present the results of heat flux estimates from the CBC on the TAG hydrothermal mound and discuss the temporal variation of heat flux and its possible causes.

## 2. TAG Hydrothermal Mound

[6] The TAG hydrothermal mound was discovered in 1985 [*Rona et al.*, 1986]. It is located on the lower eastern wall of the rift valley 2.4 km east of the spreading axis at the Mid-Atlantic Ridge (26°08′N, 44°49′W). Figure 1 shows the detailed bathymetry of the TAG hydrothermal mound. The mound is about 200 m in diameter and 60–70 m high above surrounding pillow basalts. Geochronological studies suggest that hydrothermal activity began at least 50,000 years ago, and perhaps four intervals of venting intermittently occurred with durations up to 5000–6000 years over the last 25,000 years [*Lalou et al.*, 1995, 1998]. Contemporary high-temperature activity began perhaps 60 years ago after a quiescence of about 4000 years. A detailed side-scan survey shows that the TAG hydrothermal mound lies at the intersection of a younger set of NNE-trending faults parallel to the spreading axis with an older oblique set of ENE-trending faults. These faults may provide channels to feed hydrothermal fluid to the TAG hydrothermal mound [*Kleinrock and Humphris*, 1996; *White et al.*, 1998].

[7] As shown in Figure 1, there are two approximately circular, superimposed platforms on the mound. The lower platform is ~150 m in diameter at 3650–3655 m depth. A white smoker area with 1–2 m tall chimneys from which emanates zinc-rich hydrothermal fluid of temperature of 250°–300°C is located on the SE portion of this platform. This is called the "Kremlin area" [e.g., *Edmond et al.*, 1995; *Tivey et al.*, 1995]. The upper platform, ~90 m in diameter, is constructed on the NNW portion of the lower platform. On the top of this platform, there is a CBC which is 10–15 m in height and 10–20 m in diameter at the base from which discharges high-temperature fluid (~369°C) through multiple clustered vent chimneys [*Edmond et al.*, 1995; *Edmonds et al.*, 1996]. In Figure 1, a depression about 30 m long and 20 m wide is identified in the eastern part of the upper platform. Although no hydrothermal activity was observed during previous studies in 1986–1990, submersible surveys carried out in 1993–1994 identified vigorous, NNE-trending black smoker venting within and along this depression [*Humphris and Kleinrock*, 1996; *Kleinrock and Humphris*, 1996; *Rona and Von Herzen*, 1996]. In the southern part of the upper platform, there is a small ridge-like topography. Although no black smoker emission was observed by the authors during the submersible *Shinkai 6500*'s dives in August 1994, the authors observed vigorous black smokers emitting from 1 m below the top along the eastern side of the ridge-line during submersible *MIR* dives in September 1994. During the submersible *Alvin* dives 6 months later, the authors noted that this had ceased. Smoker venting from ODP2 site (Figure 1) on the SE part of the mound was also observed to be more vigorous during these later dives. These are visual observations of an eastward shift of higher temperature venting over the 6-month period.

[8] Using submersibles, conductive heat flow measurements were carried out at and around the TAG hydrothermal mound [*Becker and Von Herzen*, 1996; *Becker et al.*, 1996]. On the SE side of the mound, very high values of heat flow (250–25,000 mW $m^{-2}$) were measured. Within 20 m of CBC, heat flow is extremely variable (100–100,000 mW $m^{-2}$). *Becker et al.* [1996] concluded that such high, variable heat flow values are the result of complex fluid advection in the vicinity of CBC. High heat flow was also measured near the periphery of the mound (300–3000 mW $m^{-2}$). On the other hand, a low heat flow zone (<20 mW $m^{-2}$)

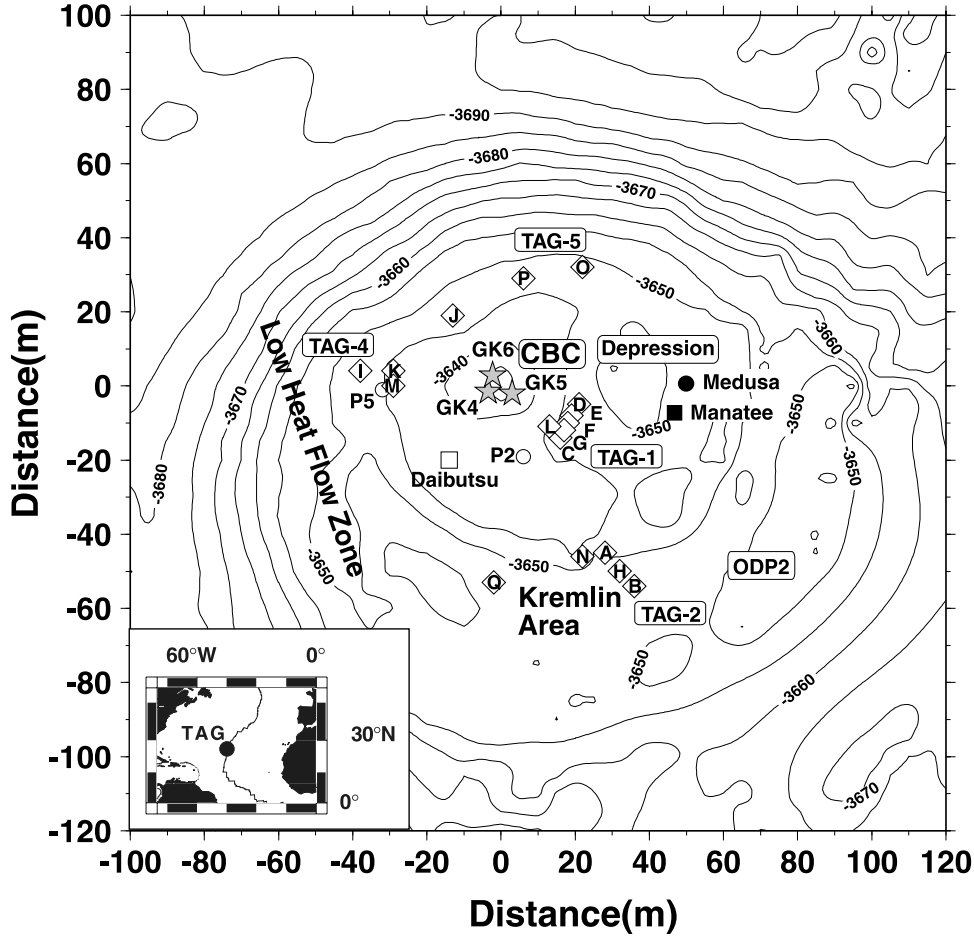


**Figure 1.** Bathymetric map (5-m contour interval) of the TAG hydrothermal mound (bathymetric data from *Humphris and Kleinrock* [1996]). Shaded stars indicate positions of Giant Kelp (GKs) (GK4, GK5, and GK6) around the CBC. The "Hobo" temperature-monitoring probe was deployed at a small black smoker vent located between GK4 and GK5. Open rectangle and circles indicate positions of Daibutsu and its probes [*Kinoshita et al.*, 1996]. Solid circle is the position of one of the Medusa hydrothermal monitoring systems described in this paper [*Schultz et al.*, 1996]. Solid rectangle indicates the position of a stationary deep seafloor observatory that monitored current velocity and direction [*Fujioka et al.*, 1997; *Kinoshita et al.*, 1998]. Diamonds with letters indicate drilling locations of ODP Leg 158 [*Humphris et al.*, 1995]. Low heat flow zone refers to conductive heat flow pattern discussed by *Becker and Von Herzen* [1996] and *Becker et al.* [1996].

extends approximately N-S on the western portion of the mound, suggesting a region of seawater entrainment into the mound [*Becker and Von Herzen*, 1996; *Becker et al.*, 1996].

[9] Heat flux due to hydrothermal discharge has been estimated at the TAG hydrothermal mound. *Rona et al.* [1993] measured temperatures inside the plume discharged from CBC using the submersible *Alvin* and estimated the heat flux at 225 ± 25 MW. *James and Elderfield* [1996] estimated total heat flux of the mound in diffuse form at 2000 MW. *Rudnicki and Elderfield* [1992] estimated heat flux at 504–940 MW from water column surveys using a towed CTD package with a nephelometer.

[10] In October–November 1994, ODP Leg 158 was carried out on the TAG hydrothermal mound [*Humphris et al.*, 1995]. From the drilling, abundant anhydrite ($CaSO_4$) was discovered below the hydrothermal discharge zones (TAG-1 and TAG-5 areas in Figure 1) of the mound, indicating that a significant quantity of seawater is entrained into the mound and that high temperatures (>150°–160°C) are currently maintained inside the mound. Chemical analyses of diffuse flow fluid indicate dynamic contemporaneous anhydrite deposition [*James and Elderfield*, 1996].

## 3. Instrumentation and Operations

### 3.1. Vertical Thermistor Array "Giant Kelp"

[11] A vertical thermistor array, designated Giant Kelp (GK), is designed to monitor the vertical temperature distribution within a plume over time. The schematic configuration of a GK is shown in Figure 2. This system consists of a flotation with three glass spheres and a data logger, a 50-m-high thermistor string with eight thermistors, and 5-m-long titanium links to an anchor weight. The system measures temperatures at each thermistor with a resolution of 0.003°C, at a sampling interval of 30 s. The

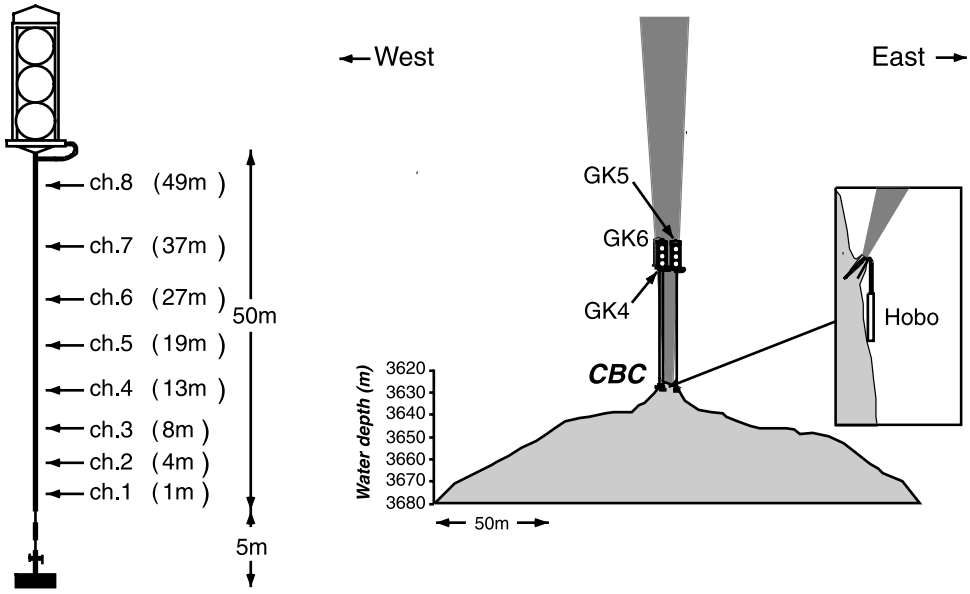


**Figure 2.** Schematic illustration of deployed Giant Kelps (GKs) and Hobo. Schematic of a vertical thermistor array GK (left). East-west cross section through CBC and deployed GKs and Hobo (right).

thermal response time of each thermistor to temperature variation is about 1 min as a result of the cable string diameter of about 1 inch, so that measured temperatures are not aliased by the sampling interval.

[12] During July to August 1994, dive observations by the submersible *Shinkai 6500* were carried out during MODE'94 (Mid-Ocean Ridge Dive Expedition) cruise at and around the TAG hydrothermal mound. During this cruise, three GKs were deployed around CBC, as illustrated in Figures 1 and 2. On August 8, one of them (GK4) was deployed on the SW wall of CBC (Figure 1). It was redeployed on 16 August since its anchor was observed to have slid down to the base of CBC. On 10 August, GK5 and GK6 were deployed on the SE and NW wall of the CBC (Figure 1), respectively. These deployed positions were determined using two methods: (1) relative positions of the GK anchors were determined from transponder navigation of *Shinkai 6500*; (2) relative positions of the GK flotation packages were determined from sonar of *Shinkai 6500*. Both were consistent, and the best estimates of relative positions are determined as follows: GK6 was 4 m north of GK4 and GK5 was 5 m east of GK4 (the relative positions are estimated to have a precision of about 1 m). The water depth of each GK anchor was determined from the depth gauge of *Shinkai 6500* as given in Table 1 (the water depths have a relative precision of about 1 m). From videotape recordings, we estimated the diameter of the top of CBC as ~3 m. This CBC diameter and geometrical consideration among GK positions indicate that all GKs were situated within 4 m of the center of CBC.

[13] The GKs are each supported by the buoyancy force of three glass spheres (the diameter and buoyancy of each glass sphere are 0.43 m and 25 kg, respectively). A horizontal current would force the GK moorings to incline by the induced drag force. Assuming that the drag force acts on three glass spheres only, we can calculate an inclination angle of the GK moorings from a simple force balance. In the case that the horizontal current is 0.2 m $s^{-1}$, the inclination angle is calculated as ~0.6°, assuming that the kinematic viscosity of seawater $\nu = 1.83 \times 10^{-6}$ $m^2$ $s^{-1}$ [*Kaye and Laby*, 1986]. *Kinoshita et al.* [1998] indicated that the typical range of horizontal current was up to 0.2 m $s^{-1}$ at TAG hydrothermal mound. Considering the cable and other hardware comprising the mooring, we estimate that the tilt angle did not exceed 1°. Therefore we can assume that the GKs remained essentially vertical and that the relative thermistor depths did not change.

[14] The GKs were recovered using the submersible *Alvin* during a joint US-UK expedition to the TAG hydrothermal mound on 28 February (GK4 and GK6) and on 3 March, 1995 (GK5).

### 3.2. Long-Term High-Temperature Monitoring Probe "Hobo"

[15] A small high-temperature monitoring probe, designated Hobo, is designed to measure temperature of hydrothermal fluid just before discharging from a hydrothermal vent. The schematic deployment is shown in Figure 2. It is made of titanium, and its length is 60 cm. The data logger is installed inside a small pressure case at the end of the probe, and a temperature sensor with an accuracy of 1.2°C is installed at the tip of the probe. Sampling interval was

**Table 1.** Estimated Height of Giant Kelp Thermistors Above Top of CBC[a]

| Sensor | Height above weight of GK, m | Height above top of CBC, m | | |
|---|---|---|---|---|
| | | GK4 | GK5 | GK6 |
| ch.1 | 6 | −2 | −3 | 1 |
| ch.2 | 9 | 1 | 0 | 4 |
| ch.3 | 13 | 5 | 4 | 8 |
| ch.4 | 18 | 10 | 9 | 13 |
| ch.5 | 24 | 16 | 15 | 19 |
| ch.6 | 32 | 24 | 23 | 27 |
| ch.7 | 42 | 34 | 33 | 37 |
| ch.8 | 54 | 46 | 45 | 49 |

[a]Note: water depth of top of CBC is 3625 m.

selected as 4.8 hours (five measurements per day) for this measurement.

[16] On 16 August 1994, Hobo was deployed in one of the black smokers of CBC between GK4 and GK5 (Figure 1). This vent is about 10 cm in diameter. Hobo was recovered using the submersible *Alvin* on 1 March 1995.

## 4. Plume Model in Stable Environment With Linear Density Stratification

[17] In previous heat flux estimates using a thermistor array [*Little et al.*, 1987; *Bemis et al.*, 1993], a simple plume model [*Fischer et al.*, 1979] was applied. This idealized model assumes that a single plume discharges into stable seawater with a uniform density. In the real ocean, density stratification affects the temperature, velocity, and width of the rising plume and causes the plume to extend horizontally at a height where the velocity of the rising plume vanishes. In the case of ambient fluid with linear density stratification, *Morton et al.* [1956] presented theoretical and experimental results for the temperature distribution and geometry of such a plume. In Morton's plume model, the mean excess temperature distribution within the plume is expressed as a function of the initial specific buoyancy flux, the vertical distance above the vent orifice, the horizontal offset from the plume centerline, and the buoyancy frequency of the ambient fluid. *Morton et al.* [1956] demonstrated that real plumes venting through a finite diameter orifice may be characterized as having a virtual height origin below the vent orifice. The following plume model, for which the plume fluid is discharged into a stable, density-stratified environment, is based on their results.

[18] We define the parameters related to the vertical distance above the vent orifice as [*Morton et al.*, 1956]

$$x_1(z) = \frac{\alpha^{1/2} N^{3/4}}{0.410 B_0^{1/4}} (z + z_0), \tag{1}$$

where $x_1(z)$ is a nondimensional parameter related to vertical distance above the virtual origin, $z$ is the vertical distance above the vent orifice, $z_0$ is the virtual height from the virtual origin to the orifice, $\alpha$ is the entrainment rate of seawater into the plume, $B_0$ is the initial buoyancy flux, and $N$ is the buoyancy frequency given as [*Eckart*, 1962; *Dera*, 1992]

$$N = \sqrt{-\frac{g}{\rho_a}\frac{d\rho_a}{dz} - \frac{g^2}{C^2}}, \tag{2}$$

where $\rho_a$, $d\rho_a/dz$, and $C$ are in situ density, density gradient (assumed uniform), and sound velocity, respectively, of ambient seawater, and $g$ is the gravitational acceleration. Theterminal height, $z_{max}$, where the plume extends horizontally is given as [*Turner*, 1986; *Turner and Campbell*, 1987]

$$z_{max} = 3.8 B_0^{1/4} N^{-3/4}. \tag{3}$$

[19] This corresponds to $x_1 = 2.8$ [*Morton et al.*, 1956]. The mean temperature along the plume centerline is given as

$$T_c(z) = \frac{0.819 B_0^{1/4} N^{5/4}}{a g \alpha^{1/2}} \frac{f(z)}{w(z)}, \tag{4}$$

where

$$f(z) = 1 - 0.1368[x_1(z)]^{8/3} + 0.0005[x_1(z)]^{16/3} - \cdots, \tag{5}$$

$$w(z) = 0.3649[x_1(z)]^{5/3} - 0.0025[x_1(z)]^{13/3} + \cdots, \tag{6}$$

and $a$ is the thermal expansion coefficient of seawater. The horizontal temperature distribution, $T(z, r)$, across the plume at the height $z$ is given as

$$T(z, r) = T_c(z) \exp\left[-80\left(\frac{r}{z + z_0}\right)^2\right], \tag{7}$$

where $r$ is the horizontal offset from the plume centerline. This equation indicates that the horizontal temperature distribution across the plume is Gaussian, with the highest temperature at the centerline.

[20] The heat flux, $H$, from a vent as a function of the initial buoyancy flux is [*Fischer et al.*, 1979; *Turner and Campbell*, 1987]

$$H = \frac{\rho c_p B_0}{a g}, \tag{8}$$

in which $\rho$ and $c_p$ are the density and specific heat of hydrothermal fluid at constant pressure, respectively. In this study, physical properties of hydrothermal fluid, the gravity cceleration, and buoyancy frequency are defined as $\rho$ = 1043 kg m$^{-3}$, $c_p$ = 4100 J kg$^{-1}$ K$^{-1}$, $a = 1.48 \times 10^{-4}$°C$^{-1}$, $\alpha$ = 0.093 (nondimensional parameter), $g$ = 9.8 m s$^{-2}$, and $N = 8.96 \times 10^{-4}$ s$^{-1}$, which was obtained from the conductivity, temperature, depth, and velocity (CTDV) system mounted on the submersible *Shinkai 6500*.

## 5. Method to Estimate Heat Flux

[21] To estimate heat flux applying the plume model described above, the mean plume temperature anomaly relative to ambient seawater at the height of the thermistor arrays must be known. In the following, we discuss temperatures measured with GKs and give constraints for heat flux estimates.

### 5.1. Temperatures Measured With GKS

[22] Figure 3 shows an example of temperatures measured with GKs. These are temperature anomalies relative to ambient seawater (about 2.7°C), and each temperature trace is offset by 2°C to avoid overlaps. Since hydrothermal effluent discharged from black smoker vents at the wall of CBC as well as from inside the interior of CBC, temperature anomalies were measured at sensors that were situated below the top of CBC (Table 1). These peripheral flows were advected into the main CBC plume, but made up only a minor component of the total plume volume. Consequently, we assume in the analysis below that the CBC plume is discharged from a single vent.

[23] Over the observation period, two typical characteristics are apparent: (1) amplitudes of temperature anomalies decrease with height above the top of CBC; (2) maximum temperature anomalies of the upper three or four thermistors occurred periodically and nearly simultaneously across the array approximately every 6 hours (intervals "A" in Figure 4). In contrast, maximum temperature anomalies of the lower

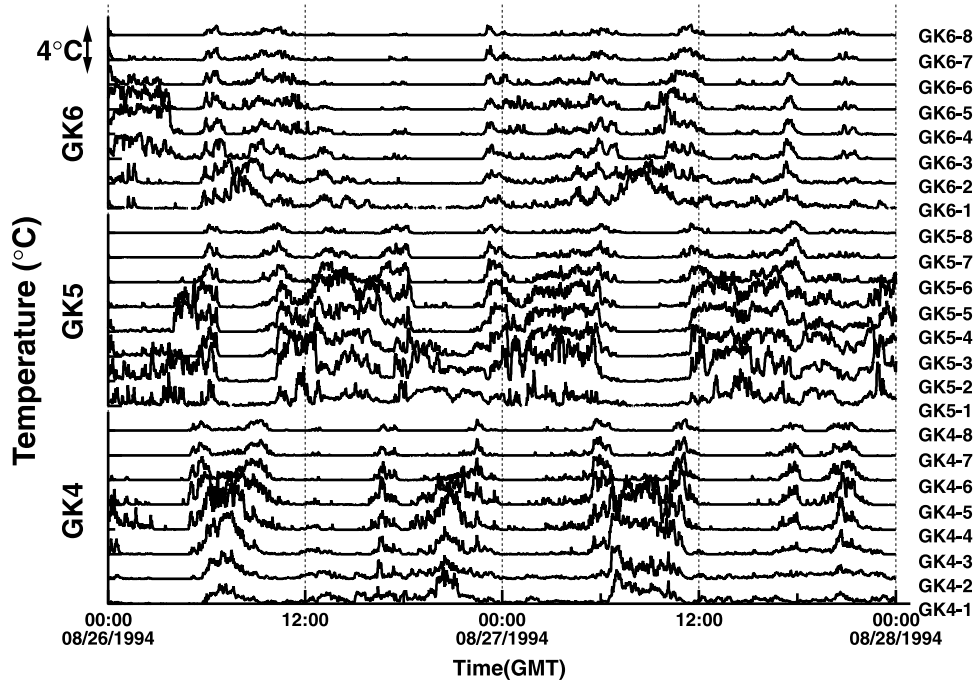


**Figure 3.** Examples of temperatures measured every 30 s by Giant Kelps (GKs) during 26–28 August 1994. Records for each GK are arranged in order of height, following Figure 2.

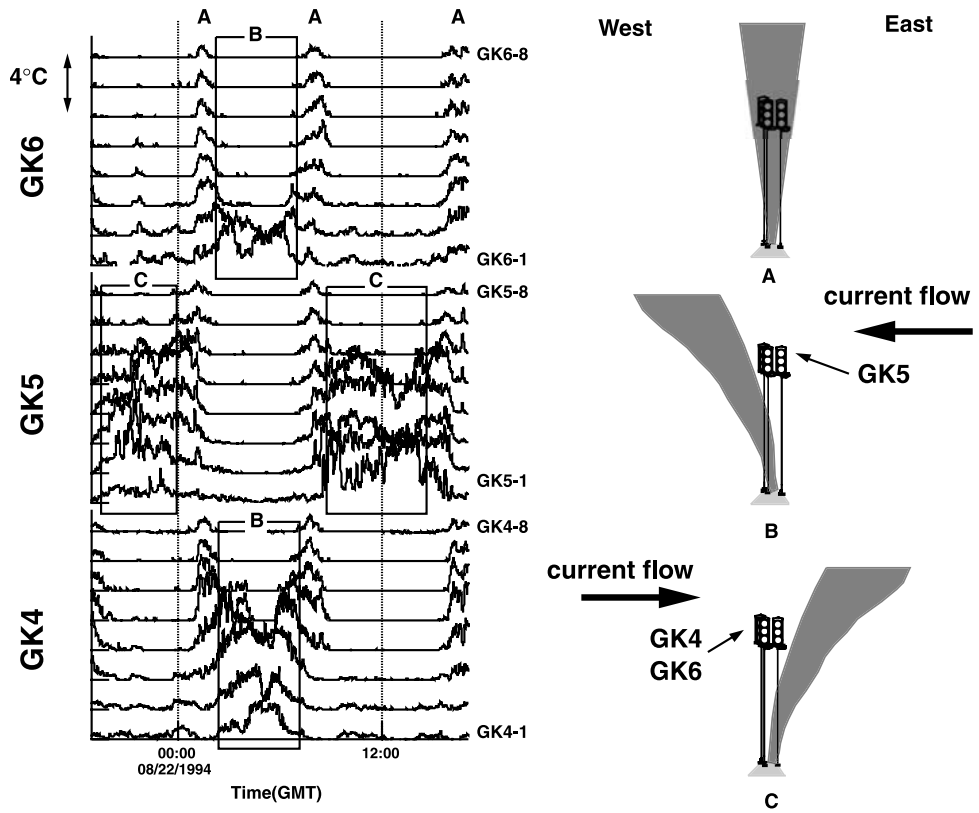


**Figure 4.** Schematic illustrations of plume movements due to tidal current. During weak current flow, the plume rose vertically (right top) and all the Giant Kelps (GKs) observed temperature anomalies in upper thermistors (period "A" in left figure). During the strong westward current (right middle), temperature anomalies are observed by GK4 and GK6 in the lower thermistors (period "B" in left top and bottom). In contrast, temperature anomalies were observed in lower thermistors of GK5 (period "C" in left middle) during the eastward current (right bottom).

four thermistors occurred periodically approximately every 12 hours, and the phase of temperature anomalies measured with GK5 was displaced about a half cycle from those measured with GK4 and GK6. At the TAG hydrothermal mound, bottom water current velocities and directions were monitored at a location east of the depression (Figure 1) from 5 to 21 August 1994 [*Kinoshita et al.*, 1998; *Fujioka et al.*, 1997]. Comparing GKs data with the current data, *Kinoshita et al.* [1998] indicated that the temporal pattern of the temperature anomalies was caused by the change in direction of tidally modulated current flow, as illustrated in Figure 4. They also indicated that a current flow with high velocity yielded temperature anomalies at the lower thermistors of GKs, and a current flow with low velocity caused temperature anomalies at the upper thermistors of GKs.

[24] In order to estimate heat flux of CBC, we need to determine the mean temperature anomaly distribution within the CBC plume. For GK measurements each thermistor has a thermal response time of about 1 min. Temperatures measured within the plume are regarded as the mean temperature at that position because most of the high-frequency variation caused by turbulent flow was significantly attenuated by this low-pass filter.

[25] The precise positions within the plume of the GK thermistors remain uncertain. In previous heat flux estimates, *Little et al.* [1987] calculated average temperatures from instantaneous maximum temperatures measured within the plume and assumed that it was measured at the plume centerline. *Bemis et al.* [1993] used two methods to obtain the average temperature at the plume centerline. One is that an average temperature at the plume centerline was calculated by using an empirical relation of plume temperature obtained by laboratory experiments as $1.5 < T_{max}/T_c < 2.5$, where $T_{max}$ and $T_c$ are the maximum temperatures measured within the plume and the average temperature at the plume centerline, respectively [*Papanicolaou and List*, 1987]. The other is that an average plume temperature at the centerline was calculated by two methods: first, average temperature was calculated from temperatures measured within the plume. Assuming that the average plume temperature was measured at some constant horizontal offset from plume centerline, the average temperature at the plume centerline was calculated using equation (7) described in the previous section. In this calculation, two horizontal offsets from plume centerline were assumed: (1) the average temperature was assumed to be measured at $r = 0.077z$; (2) the horizontal offset from the plume centerline was calculated from the ratio of two temperatures measured at different heights.

[26] As mentioned in section 3.1, all GKs were located within 4 m of the center of CBC. If the CBC plume was discharged into a stagnant ambient environment, a geometrical consideration of the diameter of the top of CBC (~3 m) and the location of each GK implies that the upper three thermistors of all GKs were wholly located within the plume since the spreading rate (0.112, *Morton et al.* [1956]) of a plume rising in a stratified density environment has a radius of ~4.1 m at height of 23 m above the top of CBC. This suggests that intervals "A" in Figure 4 were attained as a result of a zero or weak current condition that allowed the CBC plume to rise nearly vertically. However, the positions of GKs relative to the plume centerline remain unknown. Therefore we assumed that maximum temperatures of the upper three thermistors of each GK during periods such as intervals "A" in Figure 4 were measured at a uniform horizontal offset from the plume centerline (in section 6, we will indicate that this assumption is sufficiently satisfied). In the heat flux estimate, thus we first selected such intervals and then obtained the maximum temperatures at individual thermistors over each measurement period. Two unknown variables $B_0$ and $r$ were calculated by inversion from maximum temperatures at the upper three thermistors of all GKs during the same interval, and then heat flux was calculated using equation (8). In this estimate, the virtual height $z_0$ was estimated as discussed below.

### 5.2. Geometrical Consideration for Virtual Height of CBC

[27] It is important to estimate the virtual height correctly to avoid errors in the estimated heat flux. From videotape recordings recorded by the submersible *Shinkai 6500*, the diameter of top of CBC was estimated at ~3 m. *Morton et al.* [1956] estimated the virtual height of a plume discharged from a vent orifice 1.4 cm in radius as 5.19 cm. Using equation (7), this virtual height is located at a point where an isodilute line of plume temperature 0.3% of the centerline temperature converges. Assuming that this condition also applies at the radius of CBC (1.5 m), the virtual height of CBC is estimated at 5.6 m, which was used in our heat flux calculations.

## 6. Results

[28] Two hundred and ninety-three intervals of temperature anomaly measured simultaneously by all GKs were selected and 115 heat flux values were estimated. Figure 5 shows an example of the heat flux estimate for the same selected interval (2252 on 4 September to 0240 on 5 September 1994). The open circles show maximum temperatures measured by the lower five thermistors of each GK within the interval selected. The solid circles indicate the temperature maxima measured by the upper three thermistors of each GK. It is the set of measurements that was used to estimate heat flux. The dashed and thick lines indicate the best fit temperatures at estimated horizontal offset $r$ and the centerline temperatures inferred, respectively. Temperature profiles calculated at the estimated horizontal offset optimally fit to temperatures measured by the upper three thermistors of GK.

[29] Figure 6 shows time series plots of estimated heat flux values and horizontal offsets of each GK from the CBC plume centerline. The error bar in each plot indicates the standard deviation of the estimated value. The thick line in the bottom figure indicates the best linear least squares fit, and the dashed lines indicate the 95% confidence limits. The thick line in the upper three figures is the mean value of the estimated horizontal offset for each GK. These average values are 2.1 ± 0.4 m for GK4, 2.3 ± 0.3 m for GK5, and 2.9 ± 0.4 m for GK6, indicating that GK6 was located slightly more distant from the center of CBC than other two GKs. There are no significant trends in these horizontal GK offsets, suggesting that all GKs remained at the same initially deployed positions over the measurement period.

[30] When all the results are plotted versus time, a gradual decrease in heat flux is apparent (Figure 6d). We have tested

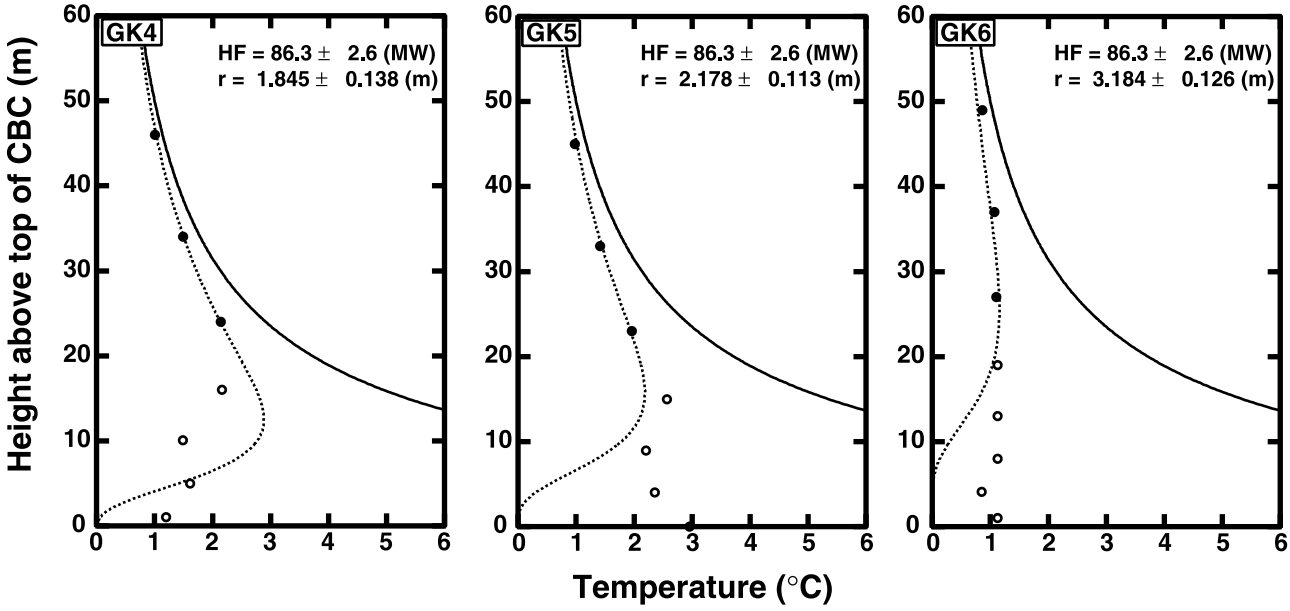


**Figure 5.** Examples of results of estimated heat flux and horizontal offsets from the plume centerline (selected interval is from 2252 on 4 September to 0240 on 5 September 1994). Open circles indicate maximum temperatures measured at lower thermistor of each Giant Kelp (GK) during the interval. Solid circles are maximum temperatures at upper thermistors of GK and were used in heat flux estimate. Dashed and solid lines indicate best fit profiles for maximum observed temperatures and temperature profiles estimated at the plume centerline, respectively.

for the statistic significance of this downward trend. Spearman's rank-order correlation coefficient [*Wampold and Drew*, 1990], a nonparametric method to test the relationship between data sets, shows a strong negative correlation between the passage of time and the estimated heat flux values (number of data $n = 115$, Spearman's rank-order correlation coefficient $R_s = -0.595$, and significance probability $P < 0.0001$). A linear fit of calculated heat flux values shows that the heat flux decreased from 86 to 55 MW over the measurement period (the rate of decrease in heat flux is 0.17 MW $d^{-1}$). To evaluate the goodness of fit, we applied a Kolmogorov-Smirnov statistic [*Hoel*, 1971] to the residual values between estimated and predicted heat flux values. The result shows that the residual values follow a normal distribution with a standard deviation of 11.3 MW (number of data $n = 115$, test statistic $D_n = 0.041$, and critical value of significance level of 0.05 $D = 0.127$).

[31] A temporal change in an ambient environmental condition such as the vertical density distribution can lead to an apparent change in the estimated heat flux. In order to assess this possibility, we calculated heat flux using a buoyancy frequency value 20% different from that used originally ($8.96 \times 10^{-4}$ $s^{-1}$). This calculation yields only 1% difference in the heat flux value calculated using the original buoyancy frequency value. The downward trend in CBC advective heat flux is therefore taken to be a robust, statistically significant feature that cannot reasonably be attributed to changes in water column stratification.

[32] In heat flux estimates derived from thermistor array data, the temperature dependence of the physical properties of seawater and the uncertainty of thermistor position within the plume may yield significant uncertainty in estimated heat flux. When high-temperature hydrothermal fluid discharges into cold seawater, thermal properties of the fluid change abruptly. Comparing heat flux values estimated from the simple plume model [*Fischer et al.*, 1979] with that from a plume model accommodating nonlinear temperature-dependent thermal properties of seawater, *Little et al.* [1987] indicated a difference of about 20% (2.76 versus 3.40 MW, respectively).

[33] To estimate heat flux uncertainty as a result of uncertainty in measurement position, *Bemis et al.* [1993] reported that a height uncertainty of ±1 m from the vent orifice results in an uncertainty of 8% in the heat flux estimate using the simple plume model. A greater heat flux uncertainty results from that caused by the uncertainty in horizontal offset from the plume centerline. In the present study, the horizontal offset between each GK and the CBC plume centerline was estimated assuming that GK strings were parallel to the CBC plume centerline. Maximum temperatures were measured by the upper three thermistors of all GKs within each selected interval. In order to assess

**Figure 6.** (opposite) Results of estimates in heat flux and horizontal offset of each Giant Kelp (GK). (a) Estimated horizontal offset for GK6 from plume centerline. Solid line indicates the average value over the measurement period (2.9 m). (b) Estimated horizontal offset for GK5 from plume centerline. Solid line indicates the average value over the measurement period (2.3 m). (c) Estimated horizontal offset for GK4 from plume centerline. Solid line indicates the average value over the measurement period (2.1 m). (d) Estimated heat flux of CBC. Solid lines indicate a linear fitting by least squares method. Dashed line indicates 95% of confidence limits on the linear fitting line.

the appropriateness of this assumption, we simulated the streamlines of the rising plume using *Middleton*'s [1986] plume model for a plume discharging into a density-stratified water column in which there is a horizontal current of constant velocity. This cross flow affects the plume centerline track. The temperature distribution within a plume rising in such a constant cross flow under conditions of density stratification is described by equation (7).

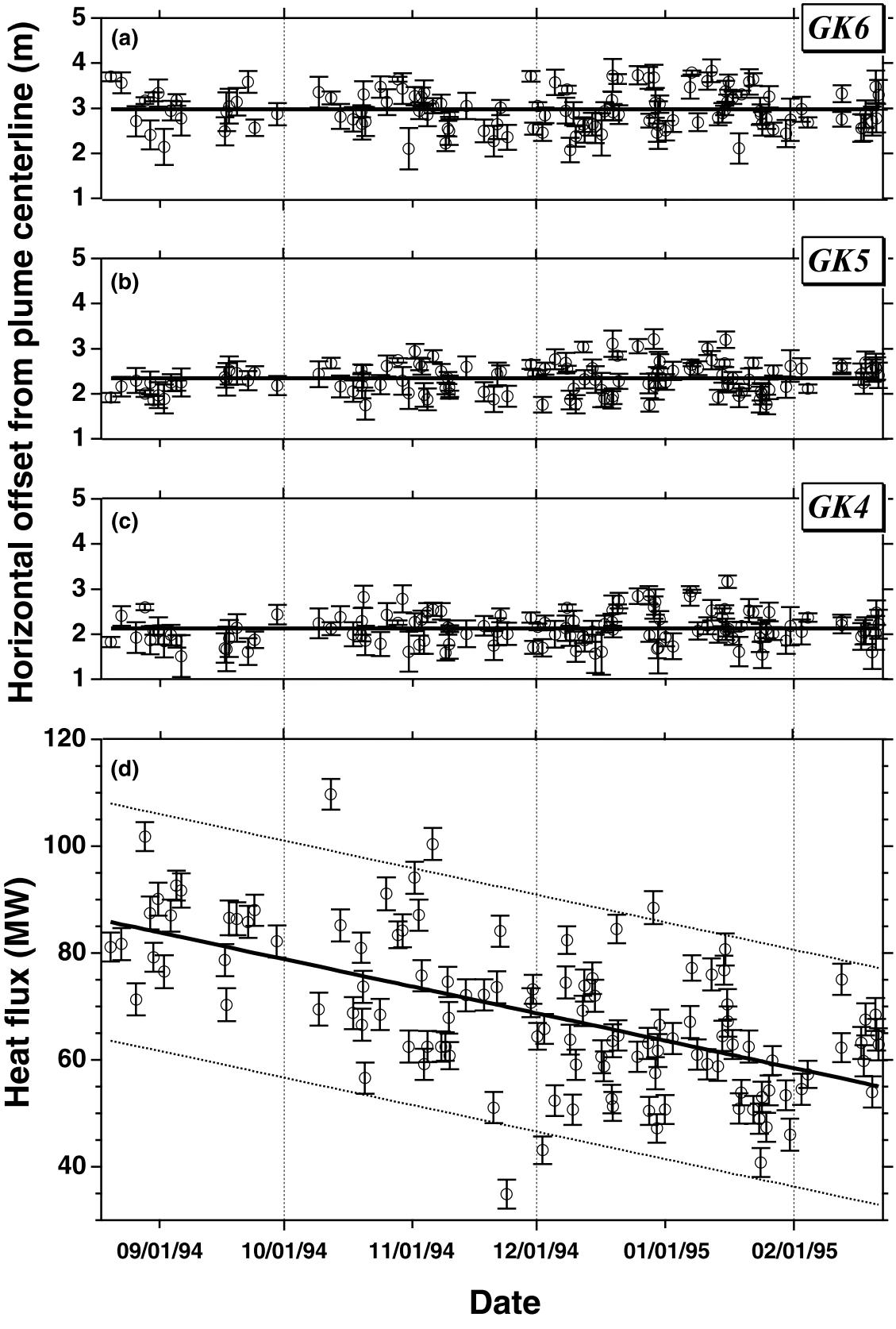

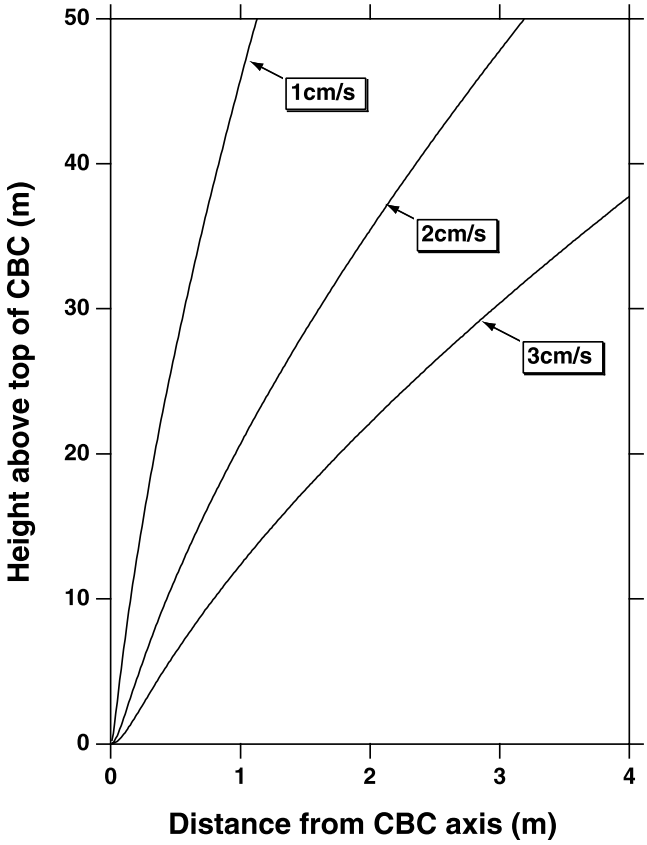


**Figure 7.** Simulated plume centerline tracks at various flow rates of cross flow with stratified density.

[34] Figure 7 shows the track of the centerline of the CBC plume simulated by *Middleton*'s [1986] plume model in cross flows ranging from 1 to 3 cm $s^{-1}$. We have assumed a heat flux of 85 MW in this simulation, which is consistent with that estimated as the baseline heat flux during the first 16 days of GK measurement at TAG. Other model parameters are $\rho = 1043$ kg $m^{-3}$, $c_p = 4100$ J $kg^{-1}$ $K^{-1}$, $a = 1.48 \times 10^{-4}$°$C^{-1}$, $g = 9.8$ m $s^{-2}$, $N = 8.96 \times 10^{-4}$ $s^{-1}$. In cross flow of 1 cm $s^{-1}$, the simulated plume centerline gradually shifts by 1.4 m at 50 m above the CBC top. In cross flow of 3 cm $s^{-1}$, surprisingly, the simulated plume centerline shifts by 3 m at only 25 m above the CBC top. Figure 8 shows the simulated temperature profiles along each GK string. In these simulations, the average value of estimated horizontal offsets between each GK and plume centerline is used (2.1 m for GK4, 2.3 m for GK5, and 2.9 m for GK6). Numbers noted on simulated temperature profiles indicate the velocity of the cross flow (positive numbers indicate that assumed cross flow flows in the direction from CBC to GK, and negative numbers indicate opposite cross flow direction). The measured temperatures (open circles) tend to plot between the profiles for 1–2 cm $s^{-1}$ cross flow, lending support to our data selection criteria. This evaluation suggests that the dispersion of estimated heat flux may be attributed to weak cross flow that can slightly bend the CBC plume track.

## 7. Discussion

[35] Although the TAG hydrothermal mound has also been visited by multiple expeditions since its discovery in

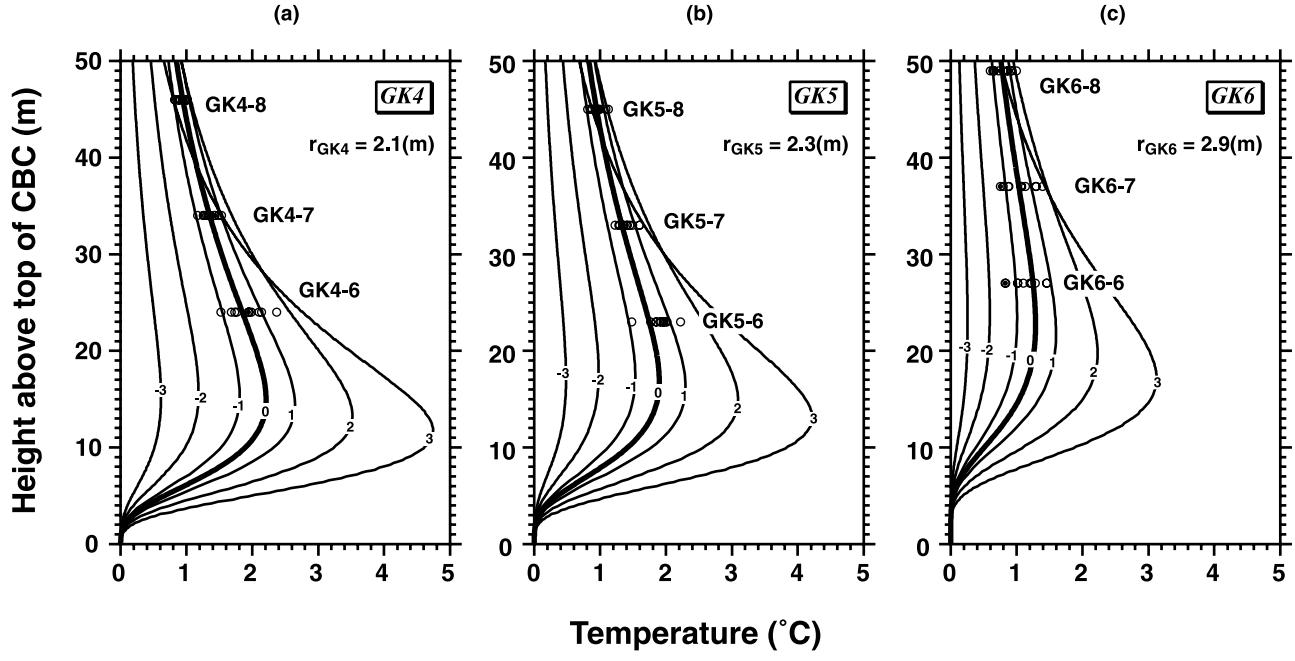


**Figure 8.** Simulated vertical temperature profiles for each Giant Kelp (GK) at various cross flow velocities within a water column with stratified density. Heat flux is assumed to be 85 MW. The $r_{GK}$ value in each figure indicates the estimated horizontal offset for the GK ((a) for GK4, (b) for GK5, and (c) for GK6). Numbers noted on each profile indicate cross flow velocities: positive values mean cross flow in the direction from CBC to the GK, and negative value indicates the opposite sense of cross flow. Maximum temperatures measured at upper three thermistors within the selected intervals from 20 August to 5 September 1994 are also plotted.

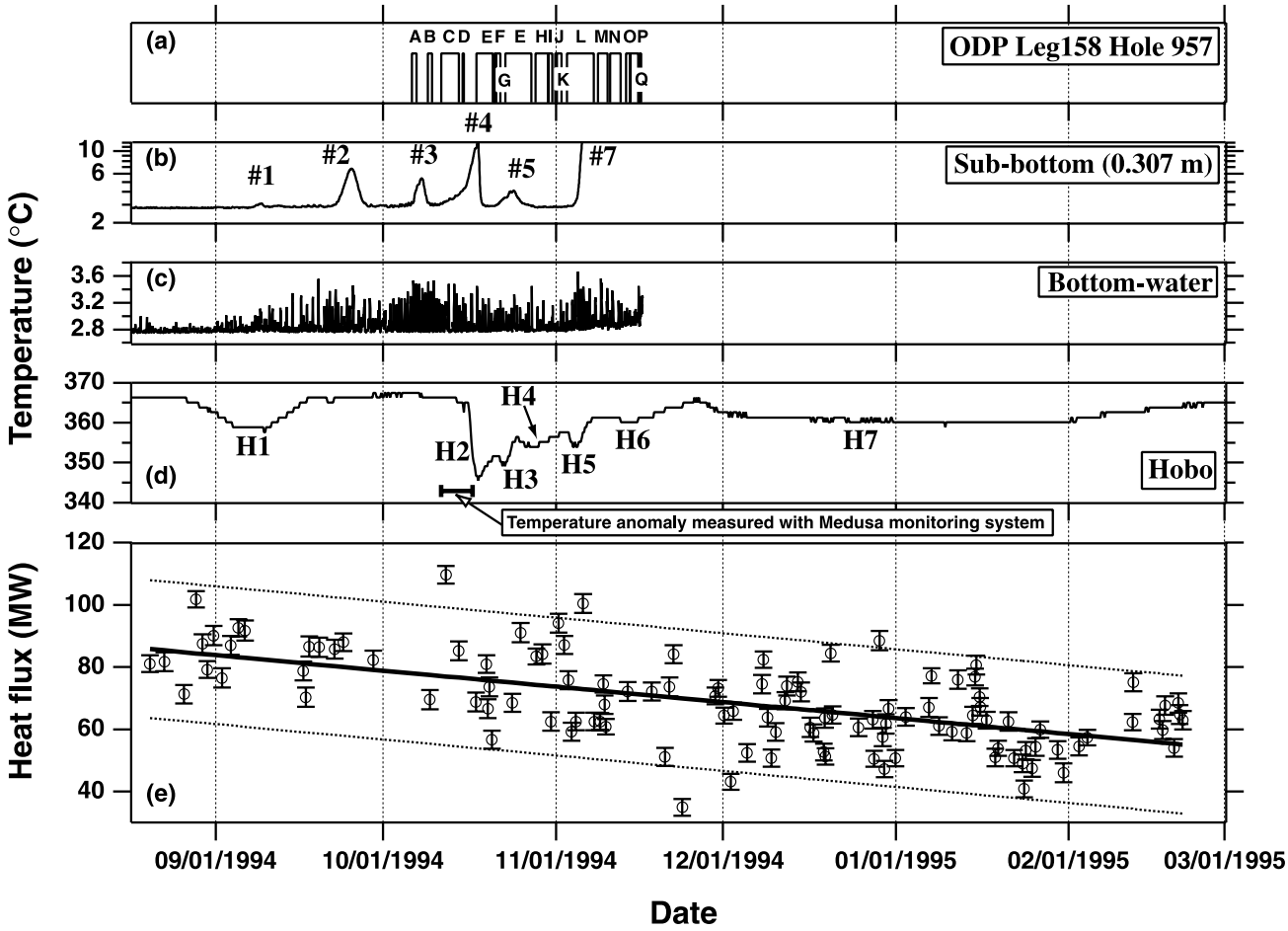


**Figure 9.** Comparison between estimated heat flux of CBC and temperatures measured with other long-term temperature-monitoring instruments. (a) Intervals of drilling of ODP Leg 158. (b) Subbottom temperature variation measured at P2 site with Daibutsu system 20 m southeast of CBC [*Kinoshita et al.*, 1996; *Goto et al.*, 2002]. Anomalous temperature increases are labeled 1, 2, 3, 4, 5, and 7. Temperature anomaly 6 was measured at P5 site within the low heat flow zone. (c) Bottom water temperature variation measured with Daibutsu system 20 m southeast of CBC [*Kinoshita et al.*, 1996; *Goto et al.*, 2002]. (d) Temperature of fluid at CBC. Anomalous temperature decreases are labeled as "H." An interval that Medusa hydrothermal monitoring system measured an anomalous temperature excursion is also shown [*Schultz et al.*, 1996]. (e) Estimated heat flux of CBC. Solid line indicates a linear fitting by least squares method. Dashed line indicates 95% confidence limits on the best-fitting line.

1985, quantitative data on long-term (greater than few weeks) plume variability is sparse, supplemented by anecdotal observations. The water column measurements relevant to total (focused and diffuse) heat flux of 504–940 MW in 1988 in the work of *Rudnicki and Elderfield* [1992] cannot be compared directly with the focused CBC plume measurements in the work of *Rona et al.* [1993] and in the present study. During the submersible *Shinkai 6500* dives carried out in August 1994, however, some effluent layers originating from hydrothermal activity of the TAG hydrothermal mound were observed at the same water depths as *Rudnicki and Elderfield* [1992], suggesting a similar total heat flux [*Goto et al.*, 1999].

[36] It is also likely that crustal pore water flow, and hence hydrothermal vent flux, varies at higher frequencies, particularly at tidal periods. *Schultz et al.* [1996] showed direct evidence for tidal variability in the diffuse flux at one site on the TAG hydrothermal mound. Tidal modulation in the GK data may be obscured by the tidal modulation of the plume location with respect to the GK arrays.

### 7.1. Heat Flux Decrease at CBC

[37] Time series plots of estimated heat flux indicates a decrease over the measurement period, as shown in Figure 6. During this period, including the drilling period of ODP Leg 158, other long-term instruments measured some anomalous signals of hydrothermal activity (Figure 9). Before commencement of drilling during ODP Leg 158, Hobo measured a decrease in the temperature of CBC fluid (H1 in Figure 9d). While this anomalous temperature decrease was measured, a long-term temperature-monitoring system "Daibutsu" measured the beginning of an increase in the bottom water temperature (Figure 9c) and three anomalous subbottom temperature increases (numbers 1–3 in Figure 9b) at the P2 site 20 m southeast of CBC (Figure 1). These observations suggest a natural temporal change in the fluid flow pattern

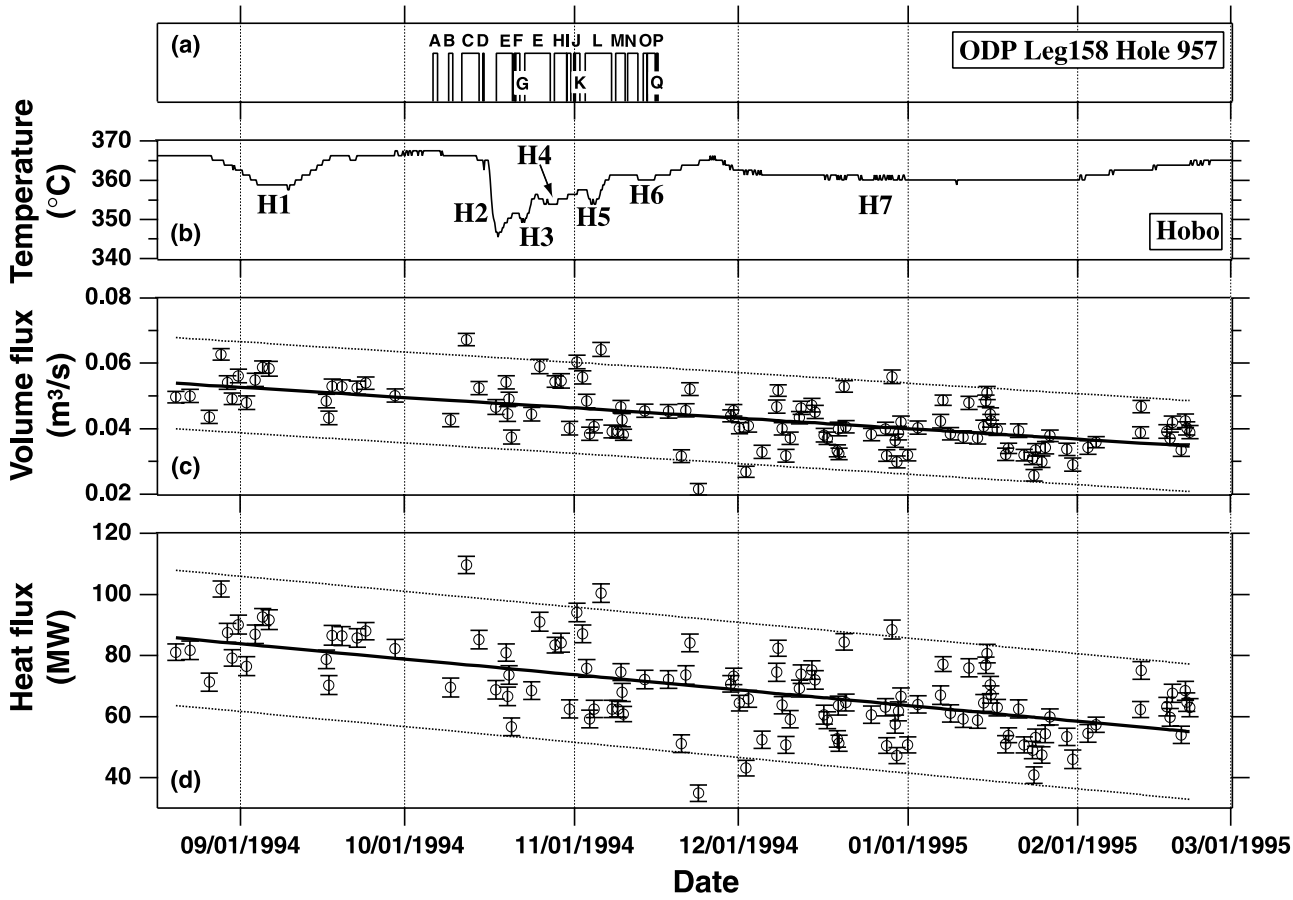


**Figure 10.** Comparison between estimated heat flux and fluid volume flux. (a) Intervals of drilling of ODP Leg 158. (b) Temperature of fluid at CBC. Anomalous temperature decreases are labeled as "H" [*Kinoshita et al.*, 1996; *Goto et al.*, 2002]. (c) Estimated volume flux of CBC. Solid line indicates linear fit by least squares. Dashed line indicates 95% confidence limits on the best-fitting line. (d) Estimated heat flux of CBC. Solid lines and dashed lines as above.

inside the mound [*Kinoshita et al.*, 1996; *Goto et al.*, 2002]. During ODP drilling, Hobo measured five decreases in fluid temperature of CBC (H2–H6) and three increases in sub-bottom temperature at the P2 site (Figure 9). A Medusa hydrothermal monitoring system, deployed on the TAG mound at a point 50 m east of CBC (Figure 1), measured an anomalous temperature perturbation of the diffuse effluent (Figure 9d) [*Schultz et al.*, 1996]. *Goto et al.* [2002] indicated that these anomalies, except for H6 in Hobo data, were excited during and/or after the drilling intervals at TAG-1 site (Figure 1), the most active of the drill sites at the TAG hydrothermal mound, and presented a possible model for changes in permeability and fluid flow pattern within the mound before and during the drilling of ODP Leg 158.

[38] The heat flux, $H$, from a single vent can be expressed as

$$H = \rho c_p V \Delta T, \tag{9}$$

where $V$ is the discharging volume of hydrothermal fluid, $\Delta T$ the temperature difference between the hydrothermal fluid and ambient seawater, $\rho$ the density of the hydrothermal fluid, and $c_p$ the specific heat of the hydrothermal fluid. This equation is another expression of equation (8). During temperature decrease H2 at CBC, the fluid temperature abruptly decreased from 365.1°C to 345.5°C. Assuming that the volume flux fed to CBC from depth was constant and calculating temperature-dependent density and specific heat of the hydrothermal fluid [*Bischoff and Rosenbauer*, 1985], this temperature decrease resulted in a decrease of about 10% in heat flux at CBC, suggesting that the ODP drilling at the TAG hydrothermal mound hardly affected the CBC hydrological regime.

[39] Using equation (9), the volume flux discharged from CBC can be calculated from Hobo data, and heat flux values can be estimated (Figure 10). This figure reveals that the decrease in heat flux over the measurement period was attributed to a decrease in the volume flux of CBC (the rate of decrease in volume flux is 8.9 $m^3\ d^{-1}$, using temperature-dependent density and specific heat of the hydrothermal fluid based on the work of *Bischoff and Rosenbauer* [1985]). There are only two possible causes for a decrease in the estimated volume flux: (1) a decrease in volume flux itself fed from depth below the TAG hydrothermal mound and (2) a decrease in volume flux supplied to CBC due to some change in fluid pathway within and/or below the mound, although the end-member volume flux fed to the TAG hydrothermal mound from depth was constant.

[40] Many submersible observations have been made at the TAG hydrothermal mound since 1986. These observations have revealed that the chemical components of the high-temperature hydrothermal fluid have not changed significantly from 1986 to 1998, suggesting that the rock-water interaction of upflowing hydrothermal fluid from depth has been stable over at least 12 years [*Edmonds et al.*, 1996; *Chiba et al.*, 1999].

[41] On the other hand, multiple submersible observations indicate spatial and temporal variations of hydrothermal activity on the mound since 1986 [*Edmonds et al.*, 1996; *Humphris and Kleinrock*, 1996; *Kleinrock and Humphris*, 1996; *Rona and Von Herzen*, 1996; *Fujioka et al.*, 1999]. The observations in 1990 and 1993 indicated that the hydrothermal activity in both the CBC and Kremlin regions of the mound was weaker than that in 1986 [*Humphris and Kleinrock*, 1996; *Rona and Von Herzen*, 1996]. In 1993, new hydrothermal activity was discovered in the topographic depression a few tens of meters east of CBC [*Humphris and Kleinrock*, 1996; *Kleinrock and Humphris*, 1996; *Rona and Von Herzen*, 1996]. Although no hydrothermal activity was observed by the authors around the Daibutsu instrument (Figure 1) during the submersible *Shinkai 6500* dives in August 1994, the authors observed vigorous black smoker flow emitted there during submersible *MIR* dives the following month. Six months later, the authors observed that this black smoker flux had ceased during dives carried out in the submersible *Alvin*. Smoker venting at the ODP2 site (Figure 1) was more vigorous during the later dives. In 1998, the hydrothermal activity at CBC appeared even weaker than that from prior observations, although hydrothermal activity in the depression seemed to have increased [*Fujioka et al.*, 1999]. Results of these time series observations suggest that the magnitude of hydrothermal activity changed over time, and that the locus of hydrothermal activity shifted somewhat from the NW and SE to the NE portion of the mound.

[42] The magnitude of hydrothermal activity depends strongly on the deep heat source (depth, volume, and temperature) and fluid pathway (recharge and discharge). A change in the deep heat source likely will modify the upflowing volume of hydrothermal fluid and/or its temperature but these are probably achieved only over a considerable time. Chemical analyses of diffuse flow fluid showed dynamic contemporaneous anhydrite deposition [*James and Elderfield*, 1996; *Schultz and Elderfield*, 1997]. Anhydrite deposition and dissolution can control the permeability distribution and the resultant fluid flow pattern within the mound. Such self-sealing systems may moderate the advective heat output at the TAG hydrothermal mound. Although temperature measurements at CBC using GKs and Hobo cannot determine the origin of the decreased volume of hydrothermal fluid, it seems more likely caused by changes in fluid pathways within the TAG hydrothermal mound.

## 8. Conclusion

[43] During August 1994 to March 1995, including the period of drilling of ODP Leg 158, three 50-m-high thermistor arrays (GKs) monitored temperatures of the plume discharging from the CBC on the TAG hydrothermal mound, and one small high-temperature probe (Hobo) monitored temperature of hydrothermal fluid from a single vent at CBC. Using a plume model in which hydrothermal fluid discharges into seawater with a linear vertical density stratification, we estimate heat flux values that decreased from 86 to 55 MW over the measurement period. Hobo measured an abrupt temperature decrease of about 20°C during ODP Leg 158, but no significant change in heat flux at CBC was observed, indicating that ODP drilling at the TAG hydrothermal mound had little effect on the hydrothermal flow at CBC, although other long-term instruments deployed at the mound surface measured anomalous temperature excursions during the drilling period [*Kinoshita et al.*, 1996; *Schultz et al.*, 1996; *Goto et al.*, 2002]. The decrease in heat flux was caused by a decrease in volume flux of hydrothermal fluid from CBC, although the variation in black smoker end-member fluid volume flux fed to the TAG hydrothermal mound from depth is not known.

[44] This paper provides evidence for a natural decrease in heat flux and for natural and possibly drilling-related temperature changes in hydrothermal fluid at the TAG hydrothermal mound over a period of approximately 6 months. This study shows that long-term monitoring can detect temporal variability of hydrothermal activity over timescales of hours to months. With extension of long-term monitoring together with other data, such as measurements of the chemical composition of the hydrothermal fluid and knowledge of the underlying lithology, the evolution of the spatial and temporal fluid flow pattern within the mound may be clarified further.

[45] **Acknowledgments.** We are indebted to the expertise and efforts of the captain and crew of R/V *Yokosuka* who successfully launched and deployed the GK arrays to the seafloor in addition to supporting the submersible *Shinkai 6500* dives at TAG hydrothermal mound during MODE'94 cruise. The *Shinkai 6500* pilots, headed by Shozo Tashiro, were instrumental in precise placement of the GK arrays close to the CBC at TAG hydrothermal mound, and their recovery was carried out with great skill by the R/V *Atlantis II*/*Alvin* groups. Jim Kirklin ably assisted in all phases of the instrument preparation, deployment and recovery, and initial data analysis. We are indebted to Kantaro Fujioka, Toshitaka Gamo, Hitoshi Chiba, Harue Masuda, Osamu Matsubayashi, Robert Evans, and Peter Rona for permission to use CTDV data and their helpful discussion about fluid activity at CBC of the TAG mound. This study was supported by the Ridge Flux project of the Science and Technology Agency, Japan, the US NSF, and the UK NERC BRIDGE program. GK instrumentation development and deployments were supported in large part by NSF grant OCE-9324542. Pressure cases and data loggers of GK instrumentation were provided by the University of Cambridge Hydrothermal Laboratory (now at Cardiff University). We are also grateful to Andrew Fisher and two reviewers for reviews and comments that improved the manuscript.

## References

Becker, K., and R. P. Von Herzen, Pre-drilling observations of conductive heat flow at the TAG active mound using DSV *Alvin*, *Proc. Ocean Drill. Program Initial Rep.*, *158*, 23–29, 1996.

Becker, K., R. P. Von Herzen, J. Kirklin, R. Evans, D. Kadko, M. Kinoshita, O. Matsubayashi, R. Mills, A. Schultz, and P. A. Rona, Conductive heat flow at the TAG active hydrothermal mound: Results from 1993–1995 submersible surveys, *Geophys. Res. Lett.*, *23*, 3463–3466, 1996.

Bemis, K. G., R. P. Von Herzen, and M. J. Mottl, Geothermal heat flux from hydrothermal plumes on the Juan de Fuca Ridge, *J. Geophys. Res.*, *98*, 6351–6365, 1993.

Bischoff, J. L., and R. J. Rosenbauer, An empirical equation of state for hydrothermal seawater (3.2 percent NaCl), *Am. J. Sci.*, *285*, 725–763, 1985.

Chiba, H., H. Masuda, K. Fujioka, and MEGATRAIN Group, Chemistry and in-situ measurements of TAG and Rainbow seafloor hydrothermal fluid, Atlantic Ridge (in Japanese and English), abstract presented at the Japan Earth and Planetary Science Joint Meeting, Volcanol. Soc. of Jpn., Tokyo, 1999.

Converse, D. R., H. D. Holland, and J. M. Edmond, Flow rates in the axial hot springs of the East Pacific Rise (21°N): Implications for the heat budget and the formation of massive sulfide deposits, *Earth Planet. Sci. Lett.*, *69*, 159–175, 1984.

Dera, J., *Marine Physics*, 516 pp., Elsevier Sci., New York, 1992.

Eckart, C., The equations of motion of sea-water, in *The Sea, Ideas and Observations on Progress in the Study of the Seas*, vol. 1, edited by M. N. Hill, pp. 31–41, Wiley-Interscience, New York, 1962.

Edmond, J. M., A. C. Campbell, M. R. Palmer, G. P. Klinkhammer, C. R. German, H. N. Edmonds, H. Elderfield, G. Thompson, and R. A. Rona, Time series studies of vent fluids from the TAG and MARK sites (1986, 1990) Mid-Atlantic Ridge: A new solution chemistry model and a mechanism for Cu/Zn zonation in massive sulphide ore bodies, in *Hydrothermal Vent and Processes*, *Geol. Soc. Spec. Publ.*, vol. 87, edited by L. M. Parson, C. L. Walker, and D. R. Dixon, pp. 77–86, 1995.

Edmonds, H. N., C. R. German, D. R. H. Green, Y. Hih, T. Gamo, and J. M. Edmonds, Continuation of the hydrothermal fluid chemistry time series at TAG, and the effects of ODP drilling, *Geophys. Res. Lett.*, *23*, 3487–3489, 1996.

Fischer, H. B., E. J. List, R. C. Y. Koh, J. Imberger, and N. H. Brooks, *Mixing in Inland and Coastal Waters*, 483 pp., Academic, San Diego, Calif., 1979.

Fornari, D. J., and R. W. Embley, Tectonic and volcanic controls on hydrothermal processes at the mid-ocean ridge: An review based on near-bottom and submersible studies, in *Seafloor Hydrothermal Systems: Physical, Chemical, Biological, and Geological interactions*, *Geophys. Mongr. Ser.*, vol. 91, edited by S. E. Humphris et al., pp. 1–46, AGU, Washington, D. C., 1995.

Fornari, D. J., T. Shanks, K. L. Von Damm, T. K. P. Gregg, M. Lilley, G. Levai, A. Bray, R. M. Haymon, M. R. Perfit, and R. Lutz, Time-series temperature measurements at high-temperature hydrothermal vents, East Pacific Rise 9°49′–51′N: Evidence for monitoring a crustal cracking event, *Earth Planet. Sci. Lett.*, *160*, 419–431, 1998.

Fujioka, K., K. Kobayashi, K. Kato, M. Aoki, K. Mitsuzawa, M. Kinoshita, and A. Nishizawa, Tide-related variability of TAG hydrothermal activity observed by deep-sea monitoring system and OBSH, *Earth Planet. Sci. Lett.*, *153*, 239–250, 1997.

Fujioka, K., H. Chiba, H. Masuda, and MEGATRAIN Group, Evolution of two different hydrothermal systems in the Atlantic Ocean (in Japanese and English), abstract presented at the Japan Earth and Planetary Science Joint Meeting, Volcanol. Soc. of Jpn., Tokyo, 1999.

Ginster, U., M. J. Mottl, and R. P. Von Herzen, Heat flux from black smokers on the Endeavour and Cleft segments, Juan de Fuca Ridge, *J. Geophys. Res.*, *99*, 4937–4950, 1994.

Goto, S., M. Kinoshita, R. P. Von Herzen, T. Gamo, H. Chiba, and K. Fujioka, Time-variation of advective heat flux from the central black-smoker complex at the TAG hydrothermal mound, Mid-Atlantic Ridge (in Japanese and English), abstract presented at the Japan Earth and Planetary Science Joint Meeting, Volcanol. Soc. of Jpn., Tokyo, 1999.

Goto, S., M. Kinoshita, and R. P. Von Herzen, Geothermal constraints on the hydrological regime of the TAG hydrothermal mound, inferred from long-term monitoring, *Earth Planet. Sci. Lett.*, *203*, 149–163, 2002.

Hoel, P. G., *Introduction to Mathematical Statistics*, 4th ed., 409 pp., John Wiley, Hoboken, N. J., 1971.

Humphris, S. E., and M. C. Kleinrock, Detailed morphology of the TAG active hydrothermal mound: Insights into its formation and growth, *Geophys. Res. Lett.*, *23*, 3443–3446, 1996.

Humphris, S. E., et al., The internal structure of an active sea-floor massive sulphide deposit, *Nature*, *377*, 713–716, 1995.

James, R. H., and H. Elderfield, Chemistry of ore-forming fluids and mineral formation rates in an active hydrothermal sulfide deposit on the Mid-Atlantic Ridge, *Geology*, *24*, 1147–1150, 1996.

Kaye, G. W. C., and T. H. Laby, *Tables of Physical and Chemical Constants and Some Mathematical Functions*, 15th ed., 477 pp., Addison-Wesley-Longman, Reading, Mass., 1986.

Kinoshita, M., O. Matsubayashi, and R. P. Von Herzen, Sub-bottom temperature anomalies detected by long-term temperature monitoring at the TAG hydrothermal mound, *Geophys. Res. Lett.*, *23*, 3467–3470, 1996.

Kinoshita, M., R. P. Von Herzen, O. Matsubayashi, and K. Fujioka, Tidally-driven effluent detected by long-term temperature monitoring at the TAG hydrothermal mound, Mid-Atlantic Ridge, *Phys. Earth Planet. Inter.*, *109*, 201–212, 1998.

Kleinrock, M. C., and S. E. Humphris, Structural control on sea-floor hydrothermal activity at the TAG hydrothermal mound, *Nature*, *382*, 149–153, 1996.

Lalou, C., J.-L. Reyss, E. Brichet, P. A. Rona, and G. Thompson, Hydrothermal activity on a $10^5$-year scale at a slow-spreading ridge, TAG hydrothermal field, Mid-Atlantic Ridge 26°N, *J. Geophys. Res.*, *100*, 17,855–17,862, 1995.

Lalou, C., J. L. Reyss, and E. Brichet, Age of sub-bottom sulfide samples at the TAG active mound, *Proc. Ocean Drill. Program Sci. Results*, *158*, 111–117, 1998.

Little, S. A., K. D. Stolzenbach, and R. P. Von Herzen, Measurements of plume flow from a hydrothermal vent field, *J. Geophys. Res.*, *92*, 2587–2596, 1987.

Macdonald, K. C., Hydrothermal heat flux of the "black smoker" vents on the East Pacific Rise, *Earth Planet. Sci. Lett.*, *48*, 1–7, 1980.

Middleton, J. H., The rise of forced plumes in a stably stratified crossflow, *Boundary Layer Meteorol.*, *36*, 187–199, 1986.

Morton, B. R., G. I. Taylor, and J. S. Turner, Turbulent gravitational convection from maintained and instantaneous source, *Proc. R. Soc. London, Ser. A*, *234*, 1–23, 1956.

Papanicolaou, P. N., and E. J. List, Statistical and spectral properties of tracer concentration in round buoyant jet, *Int. J. Heat Mass Transfer*, *30*, 2059–2071, 1987.

Rona, P. A., and R. P. Von Herzen, Introduction to special section on measurements and monitoring at the TAG hydrothermal field, Mid-Atlantic Ridge, 26°N, 45°N, *Geophys. Res. Lett.*, *23*, 3427–3430, 1996.

Rona, P. A., G. Klinkhammer, T. A. Nelsen, J. H. Trefry, and H. Elderfield, Black smokers, massive sulphides and vent biota at the Mid-Atlantic Ridge, *Nature*, *321*, 33–37, 1986.

Rona, P. A., M. D. Hannington, C. V. Raman, G. Thompson, M. K. Tivey, S. E. Humphris, C. Lalou, and S. Petersen, Active and relict sea-floor hydrothermal mineralization at the TAG hydrothermal field, Mid-Atlantic Ridge, *Econ. Geol.*, *88*, 1989–2017, 1993.

Rudnicki, M. D., and H. Elderfield, Theory applied to the Mid-Atlantic Ridge hydrothermal plumes: The finite-difference approach, *J. Volcanol. Geotherm. Res.*, *50*, 161–172, 1992.

Schultz, A., and H. Elderfield, Controls on the physics and chemistry of seafloor hydrothermal circulation, *Philos. Trans. R. Soc. London, Ser. A*, *355*, 387–425, 1997.

Schultz, A., J. R. Delaney, and R. E. McDuff, On the partitioning of heat flux between diffuse and point source seafloor venting, *J. Geophys. Res.*, *97*, 12,299–12,314, 1992.

Schultz, A., P. Dickson, and H. Elderfield, Temporal variations in diffuse hydrothermal flow at TAG, *Geophys. Res. Lett.*, *23*, 3471–3474, 1996.

Tivey, M. K., S. E. Humphris, G. Thompson, M. D. Hannington, and P. A. Rona, Deducing patterns of fluid flow and mixing within the TAG active hydrothermal mound using mineralogical and geochemical data, *J. Geophys. Res.*, *100*, 12,527–12,555, 1995.

Turner, J. S., Turbulent entrainment: The development of the entrainment assumption, and its application to geophysical flows, *J. Fluid Mech.*, *173*, 431–471, 1986.

Turner, J. S., and I. H. Campbell, Temperature, density and buoyancy fluxes in "black smoker" plumes, and the criterion for buoyancy reversal, *Earth Planet. Sci. Lett.*, *86*, 85–92, 1987.

Wampold, B. E., and C. J. Drew, *Theory and Application of Statistics*, 511 pp., McGraw-Hill, New York, 1990.

White, S. N., S. E. Humphris, and M. C. Kleinrock, New observations on the distribution of past and present hydrothermal activity in the TAG Area of the Mid-Atlantic Ridge (26°08′N), *Mar. Geophys. Res.*, *20*, 41–56, 1998.

S. Goto, Earthquake Research Institute, University of Tokyo, Yayoi 1-1-1, Bunkyo-ku, Tokyo 113-0032, Japan. (sgoto@eri.u-tokyo.ac.jp)

M. Kinoshita, Japan Marine Science and Technology Center, Natsuhima-cho 2-15, Yokosuka, Kanagawa 237-0061, Japan.

A. Schultz, School of Earth Sciences, Cardiff University, P.O. Box 914, Cardiff CF10 3YE, UK.

R. P. Von Herzen, Woods Hole Oceanographic Institution, Woods Hole, MA 02543, USA.